Supplementary Materials for

Bimolecular Reaction Dynamics in the Phenyl - Silane System: Exploring the Prototype of a Radical Substitution Mechanism

Michael Lucas, Aaron M. Thomas, Tao Yang, Ralf I. Kaiser*, Alexander M. Mebel, Diptarka Hait, Martin Head-Gordon*

This PDF file includes:

Supplementary Text
Comparison between calculated barrier height and experimental collision energy
Note on QCT calculations
Figs. S1 to S4
Tables S1 to S4
Captions for Movies S1 to S2

Other Supplementary Materials for this manuscript includes the following:

Movies S1 to S2

Supplementary Text:

We would like to discuss briefly the nomenclature of the reaction mechanism. The well-accepted reaction mechanisms at aromatic moieties were defined as nucleophilic (S_N), electrophilic (S_E), and radical substitutions (S_R). Following this nomenclature, the naming of the reaction mechanism at aliphatic moieties should also reflect the nucleophilic (S_N), electrophilic (S_E), and radical substitution (S_R) definitions with an added index '1' or '2' for a two-step (unimolecular) and one-step (bimolecular) reaction mechanism, respectively. This has been accepted by the community for the nucleophilic (S_N) and electrophilic (S_E) reactions. Presumably because there were no experiments in the early days that could distinguish unimolecular versus bimolecular, this notation has not been adopted for the radical substitution (S_R) mechanism, which has been instead been labeled as a homolytic substitution reaction (S_H). Based on the aforementioned history and definitions, together with the clear experimental evidence of a concerted (bimolecular) mechanism involving a single step, we assert that this example of a homolytic reaction mechanism should be named an S_R2 mechanism.

Comparison between calculated barrier height and experimental collision energy:

The calculated barrier height for the substitution [2a] pathway is 39.1 kJ mol^{-1} with the CCSD(T)-F12/cc-pVTZ-F12 based protocol described in the manuscript, which is slightly higher than the 38 ± 1.3 kJ mol^{-1} collision energy employed in the experiment. Experimental observation of the substitution pathway however suggests that the true reaction barrier must be strictly smaller than the collision energy. This is not a particularly problematic issue, as the theoretical barrier estimate has an uncertainty of 5 kJ mol^{-1}, bringing the estimated barrier well within the range of collision energies employed in the experiment. Nonetheless, it is useful to see if the theoretical value can be further refined.

The potential sources of error in the theoretical barrier estimate are errors in the electronic CCSD(T)-F12/cc-pVTZ-F12 energy estimates, errors in the zero-point energy (ZPE) estimate and anharmonic corrections to the molecular energy. The systems under consideration are too large for electronic structure methods more accurate than CCSD(T)-F12, but the basis set incompleteness error can be estimated. CCSD(T)-F12 yields a slightly smaller barrier of 38.8 kJ mol^{-1} with the larger cc-pVQZ-F12 basis set and subsequent extrapolation to the complete basis set (CBS) limit only marginally reduced the barrier to 38.6 kJ mol^{-1}. This suggests that there is no substantial basis set incompleteness error here (or indeed, in any of the other CCSD(T)-F12/cc-pVTZ calculations).

A more likely candidate behind the discrepancy is the ZPE estimate, as ZPE calculations with the XYGJ-OS[1] double hybrid functional yielded a barrier that was 1 kJ mol^{-1} lower. We note that this shift is rather small relative to the scale of ~10^2 kJ mol^{-1} ZPE for the species involved and is therefore not very surprising. This however does suggest that a more accurate level of theory beyond double hybrid DFT could yield slightly different numbers but such methods are computationally unfeasible at present.

Another possible factor could be anharmonic corrections to the total molecular energy, as the harmonic oscillator approximation may not be sufficiently accurate for the species involved---

[1] Zhang, I.Y., Xu, X., Jung, Y. and Goddard, W.A., 2011. A fast doubly hybrid density functional method close to chemical accuracy using a local opposite spin ansatz. *Proceedings of the National Academy of Sciences*, *108*(50), pp.19896-19900.

especially the transition state with low frequency modes. This effect however is difficult to estimate very accurately due to computational cost but is expected to be quite a bit smaller than the ZPE contribution (~5 kJ mol^{-1}). We attempted to estimate the anharmonic contribution using the transition-optimized shifted Hermite (TOSH) [2] approach with a cheaper B3LYP[3,4]/6-311G** level of theory. This contribution further lowered the barrier by a further 1.3 kJ mol^{-1}. Cumulatively therefore, all these corrections serve to marginally refine the previous barrier estimate of 39.1 kJ mol^{-1} to 36.3 kJ mol^{-1}, which is slightly lower than the experimental collision energy. The overall uncertainty of ~5 kJ mol^{-1} associated with the theoretical values however make very precise comparisons superfluous, and it is quite clear that the theoretical barrier estimate of 36.3-39.1 ± 5 kJ mol^{-1} does not indicate that the substitution reaction cannot occur under experimental conditions.

[2] Lin, C.Y., Gilbert, A.T. and Gill, P.M., 2008. Calculating molecular vibrational spectra beyond the harmonic approximation. *Theoretical Chemistry Accounts*, *120*(1-3), pp.23-35.

[3] Becke, A.D., 1993. Density-functional thermochemistry. III. The role of exact exchange. *The Journal of chemical physics*, *98*(7), pp.5648-5652.

[4] B3LYP was employed as it is a hybrid functional related to the B2PLYP double hybrid used in geometry optimizations but is considerably cheaper due to lack of a perturbative correction that is present in the latter functional.

Note on QCT Calculations:

All QCT calculations were done with 38 kJ mol^{-1} total fragment translational kinetic energy (versus the estimated 35 kJ mol^{-1} barrier height under QCT conditions).

The initial geometries for the reactant molecules were optimized at ωB97X-V/6-31+G* level of theory, and kinetic energy corresponding to zero-point energy was supplied to each vibrational normal mode (the signs of the corresponding normal mode velocities were randomly chosen, with a total of 5 sets of velocities employed per orientation). The relative orientation of the molecules was varied in order to explore various reactive conditions.

Experimental evidence appears to indicate that backward scattering is the major route to the substitution product, and the vast majority of our QCT calculations were consequently dedicated to such trajectories. An exploration of 195 forward scattering (stripping dynamics) trajectories revealed that such routes were likely not relevant (0 trajectories had substitution and only 1 had H abstraction). These trajectories were run with the phenyl radical and silane having their initial fragment velocities along separated parallel lines (which were nonetheless coplanar to the plane of the phenyl ring and orthogonal to the line connecting the center of the benzene ring to the carbon radical center, in order to maximize the radical center's interaction with silane). The perpendicular distance between the initial velocities and orientation of the silane molecule were varied, along with the signs of QCT normal mode velocities.

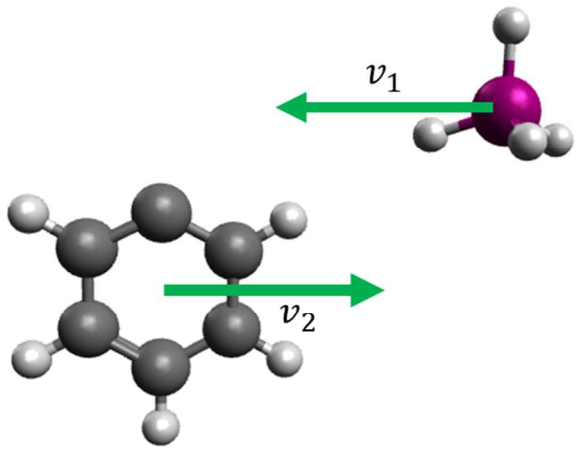

Fig S1. Representative initial positions and velocities of phenyl radical and silane for stripping dynamics.

The backward scattering dynamics were run with configurations where the silicon of the silane was initially coplanar to the phenyl ring, and closest to radical center spatially. The initial fragment velocities furthermore were along the axis connecting the Si atom to the radical center, in order to maximize the chances of head-on collision. We also constrained one of the hydrogen atoms of the silane to be coplanar with the phenyl ring, in order to have a manageable number of degrees of freedom. We can therefore define an angle θ_{HSiC} between the carbon radical center and this silicon-hydrogen (Si-H) bond, which we can vary. Other degrees of freedom (silane orientation and signs of QCT normal mode velocities) were also allowed to vary. A total of 1400 trajectories were run under such conditions for 35 θ_{HSiC} (20 trajectories per angle, with differing silane orientations and QCT velocities) to obtain Fig 4 in the manuscript.

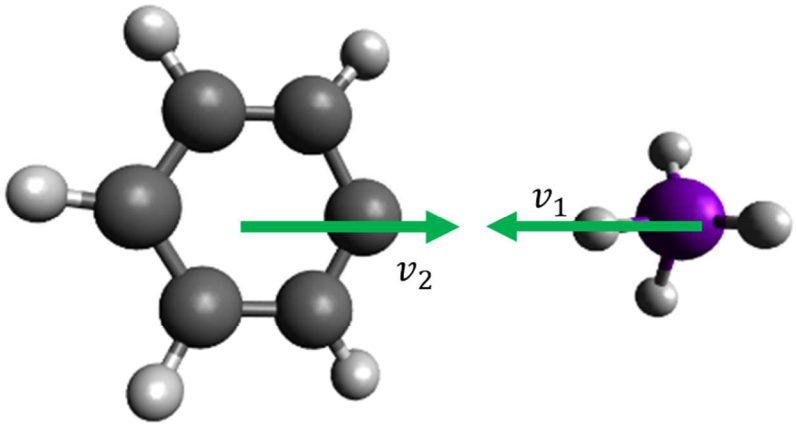

Fig S2. Representative initial positions and velocities of phenyl radical and silane for head-on collisions.

The RMS energy fluctuations in the QCT trajectories was of the order of 1 millihartree (2.5 kJ mol^{-1}), and was similar for all trajectories (including pathways that led to H abstraction as well as routes that led to substitution). This, therefore is rather unlikely to have a strong influence on the branching ratio.

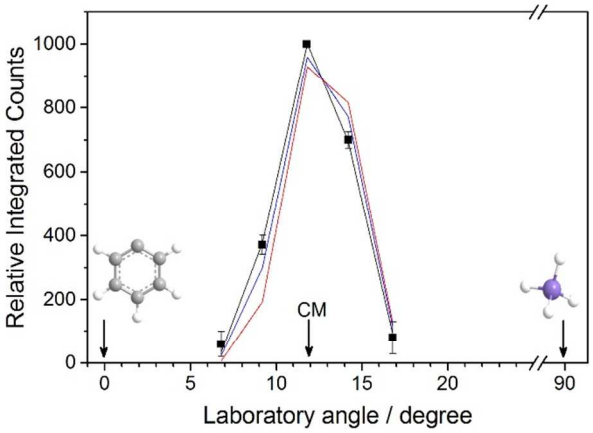

Fig. S3. Laboratory angular distribution of the crossed-beam reaction of phenyl and silane. The solid squares are the relative integrated counts of each of the recorded angles. The solid lines represents various fits from the forward-convolution routine with various degrees of backward scattering.

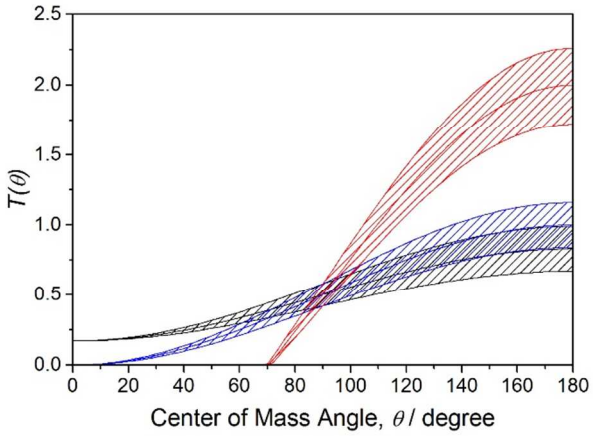

Fig. S4. Center-of-mass angular distribution of the formation of phenylsilane and atomic hydrogen from the reaction of phenyl and silane from the various fits in Fig. S1. The shaded areas represent the experimental error.

Table S1. Vibrational frequencies and geometrical parameters of the reactants, intermediates, products, and transition states, at the B2PLYP-D3/6-311G** level of theory.

Structure	Coordinates	Frequencies
C_6H_5	6 0 0.000000 0.000000 -1.322996 6 0 0.000000 1.212214 -0.631871 6 0 0.000000 -1.212214 -0.631871 6 0 0.000000 1.224667 0.770830 6 0 0.000000 -1.224667 0.770830 6 0 0.000000 0.000000 1.397670 1 0 0.000000 0.000000 -2.406247 1 0 0.000000 2.150130 -1.176133 1 0 0.000000 -2.150130 -1.176133 1 0 0.000000 2.157563 1.321479 1 0 0.000000 -2.157563 1.321479	399.3768 421.2447 600.2679 619.2476 637.4067 715.5983 817.4810 885.1210 951.5284 959.0997 989.5623 1027.1503 1055.4382 1078.5447 1180.1610 1181.9146 1310.5985 1339.0545 1467.4973 1478.4932 1590.0110 1644.0505 3182.8021 3189.4860 3203.6100 3206.0665 3215.1963
SiH_4	14 0 0.000000 0.000000 0.000070 1 0 0.000000 0.000000 -1.478347 1 0 0.000000 1.393917 0.492458 1 0 -1.207168 -0.696959 0.492458 1 0 1.207168 -0.696959 0.492458	944.8900 945.3209 945.3219 996.7993 996.8018 2280.5787 2286.0806 2286.5567 2286.5734
C_6H_5…SiH_4 complex	6 0 -0.659414 -1.221236 -0.113978 6 0 -2.053406 -1.216364 0.043443 6 0 -2.746616 -0.007788 0.121868 6 0 -2.067225 1.208661 0.044714 6 0 -0.673335 1.229552 -0.112680 6 0 -0.046712 0.007737 -0.183092 14 0 3.260773 0.000569 0.061007 1 0 -0.105223 -2.149796 -0.177665 1 0 -2.588956 -2.157238 0.104065 1 0 -3.823057 -0.013993 0.243309 1 0 -2.613408 2.143337 0.106307 1 0 -0.129790 2.164475 -0.175134 1 0 2.730748 -0.030629 1.439813 1 0 2.810710 1.228970 -0.627323 1 0 2.806807 -1.193384 -0.683098 1 0 4.741598 -0.003087 0.113975	4.8579 15.0583 23.1901 58.2763 131.9203 163.1429 399.7351 420.6372 599.5567 620.6999 629.1062 715.2203 815.8286 884.1292 931.2317 945.2964 945.8810 950.0187 957.0740 988.1503 992.8024 997.2503 1027.3828 1056.0848 1078.3775 1180.1822 1181.2770 1309.7994 1339.6947 1468.2536 1478.0251 1588.3521 1644.8416 2265.9525 2281.5599 2286.2378 2290.5806 3183.0743 3189.9745 3203.9514 3206.5572 3214.8985
C_6H_5-SiH_4, TS1 (subst.)	6 0 0.341180 1.213470 -0.034322 6 0 1.738556 1.206953 0.009523 6 0 2.435800 -0.000089 0.031677 6 0 1.738394 -1.207044 0.009540 6 0 0.341025 -1.213378 -0.034322 6 0 -0.338565 0.000093 -0.048550 14 0 -2.429994 0.000009 0.024052 1 0 -0.195753 2.153985 -0.058333 1 0 2.276487 2.148269 0.022056 1 0 3.518803 -0.000161 0.062057 1 0 2.276202 -2.148430 0.022085	489.1644*i* 41.6303 115.5333 165.9941 193.0328 259.2529 377.0299 399.9703 437.5654 618.6036 626.4255 674.4116 724.9152 815.6179 830.9444 854.4034 896.6387 953.5199 956.0530 962.7845 971.7181 998.3568 1031.1797 1069.4868 1094.6225 1184.3531 1204.3173 1329.3535 1343.7646 1463.2887 1496.7634 1603.3639 1622.0574

	1 0 -0.196029 -2.153826 -0.058362 1 0 -2.408616 -0.001195 1.510950 1 0 -2.394750 -1.302941 -0.704419 1 0 -2.394820 1.304215 -0.702183 1 0 -3.999942 -0.000071 -0.031846	1693.5201 2141.7346 2179.3480 2212.0230 3183.4103 3190.3991 3203.0506 3206.9367 3214.6476
C_6H_5-SiH_4, TS2 (abst.)	6 0 0.670003 -1.230840 0.002337 6 0 2.070538 -1.201618 -0.000917 6 0 2.745142 0.020465 -0.002416 6 0 2.034346 1.221716 -0.000849 6 0 0.633482 1.208875 0.002382 6 0 0.005164 -0.020642 0.003912 1 0 0.136017 -2.174959 0.003202 1 0 2.629357 -2.131255 -0.002309 1 0 3.828644 0.036632 -0.004932 1 0 2.565057 2.167673 -0.002180 1 0 0.070890 2.136233 0.003259 14 0 -3.237526 -0.001871 -0.001064 1 0 -3.744825 -0.832835 -1.116836 1 0 -3.760925 -0.522341 1.282542 1 0 -3.686085 1.397622 -0.185642 1 0 -1.664817 -0.038311 0.011098	524.9593*i* 10.2499 46.3666 48.7589 228.7972 287.1924 394.9611 416.4638 450.9348 609.4463 627.5771 714.8473 785.3403 831.5707 885.3090 900.5553 947.0250 950.4876 957.3624 963.7024 981.8250 1016.1813 1032.1591 1044.4359 1084.8465 1099.3024 1181.6112 1187.2165 1322.7344 1342.9566 1469.1099 1491.5344 1599.4541 1639.9520 2258.4479 2271.3759 2272.9234 3176.6557 3181.2728 3191.7657 3196.0870 3210.9162
$C_6H_5SiH_3$	6 0 0.254504 1.204476 -0.011276 6 0 1.648856 1.206786 0.003506 6 0 2.348091 0.000000 0.012286 6 0 1.648856 -1.206786 0.003506 6 0 0.254503 -1.204475 -0.011276 6 0 -0.468257 0.000000 -0.015137 14 0 -2.343682 0.000000 0.007078 1 0 -0.273888 2.152353 -0.026452 1 0 2.188154 2.146952 0.004415 1 0 3.431790 0.000000 0.021501 1 0 2.188153 -2.146952 0.004414 1 0 -0.273891 -2.152351 -0.026452 1 0 -2.870150 0.000177 1.393057 1 0 -2.848954 -1.211532 -0.679459 1 0 -2.848973 1.211350 -0.679765	32.2867 145.5670 197.6714 389.6396 394.8535 421.2965 631.9848 635.3859 664.0870 691.4637 707.1617 742.9868 860.4986 912.2189 954.7358 960.6290 964.9637 969.8236 986.3662 1015.9295 1050.8717 1101.4683 1137.3895 1187.5717 1216.7744 1325.1473 1364.6931 1465.3923 1522.3176 1616.9894 1638.7029 2256.5356 2263.8914 2268.3331 3173.7339 3174.9163 3190.1728 3200.6428 3212.2737
C_6H_6	6 0 0.000000 0.000000 1.395301 6 0 0.000000 1.208319 0.697636 6 0 0.000000 -1.208319 0.697636 6 0 0.000000 1.208319 -0.697636 6 0 0.000000 -1.208319 -0.697636 6 0 0.000000 0.000000 -1.395301 1 0 0.000000 0.000000 2.479028 1 0 0.000000 2.146888 1.239446 1 0 0.000000 -2.146888 1.239446 1 0 0.000000 2.146888 -1.239446	405.5872 406.1233 620.3571 620.3586 658.2869 685.7936 856.4775 857.6157 958.2158 958.9152 965.3137 1014.4841 1021.1956 1062.9041 1063.1276 1177.5306 1201.4949 1201.6353 1359.9392 1382.9353 1516.2032 1516.3993 1642.9268 1642.9419 3181.6731 3191.7368 3191.7557 3207.5513 3207.6040 3217.8144

	1 0 0.000000 -2.146888 -1.239446 1 0 0.000000 0.000000 -2.479028	
SiH_3	14 0 0.000000 0.000000 0.079261 1 0 0.000000 1.409953 -0.369886 1 0 1.221055 -0.704976 -0.369886 1 0 -1.221055 -0.704976 -0.369886	784.0244 955.7615 955.7643 2244.2966 2280.6846 2280.7008
CH_4	6 0 0.000000 0.000000 0.000092 1 0 0.000000 0.000000 -1.089238 1 0 0.000000 1.027016 0.362896 1 0 -0.889422 -0.513508 0.362896 1 0 0.889422 -0.513508 0.362896	1356.5283 1356.9098 1356.9116 1574.7400 1574.7421 3054.3891 3169.5256 3170.4980 3170.5005
$C_6H_5…CH_4$ complex	6 0 -0.907460 1.427669 -0.098153 6 0 -2.080701 0.720547 0.204710 6 0 -2.072009 -0.674515 0.231620 6 0 -0.901599 -1.383635 -0.041438 6 0 0.283948 -0.698516 -0.346044 6 0 0.214139 0.675294 -0.358923 1 0 -0.898568 2.510632 -0.123708 1 0 -2.994226 1.264406 0.417975 1 0 -2.982681 -1.212132 0.466612 1 0 -0.903002 -2.467738 -0.018140 1 0 1.201381 -1.233302 -0.558825 6 0 3.935841 0.073974 0.226543 1 0 4.072258 -0.457688 -0.715176 1 0 4.844621 0.626426 0.463585 1 0 3.728098 -0.641106 1.022138 1 0 3.099164 0.765592 0.135649	7.6004 24.9468 33.5107 47.4042 54.7744 92.6549 399.9671 420.9621 600.0742 619.4807 634.5575 716.3063 818.2215 885.9247 951.7371 958.1997 988.7294 1027.1773 1055.5562 1078.6183 1180.1340 1181.8180 1310.2942 1339.2256 1353.2238 1358.4946 1360.6604 1467.5977 1478.0584 1574.1724 1574.8006 1589.2639 1644.0815 3049.4082 3162.5252 3165.3988 3169.3310 3183.2528 3190.3635 3204.3210 3208.5501 3215.4773
C_6H_5-CH_4, TS1 (subst.)	6 0 0.077674 -1.214496 -0.007506 6 0 -1.320724 -1.202960 0.002352 6 0 -2.009628 0.009843 0.007521 6 0 -1.302747 1.213314 0.002267 6 0 0.094619 1.204026 -0.007685 6 0 0.765851 -0.010644 -0.014793 6 0 2.620828 -0.002442 0.007849 1 0 0.613426 -2.159167 -0.011157 1 0 -1.868904 -2.138778 0.005888 1 0 -3.093062 0.017787 0.014799 1 0 -1.837472 2.156883 0.005704 1 0 0.645857 2.139859 -0.011560 1 0 2.639862 0.328908 1.041042 1 0 2.667327 0.727771 -0.793877 1 0 2.676387 -1.062298 -0.221939 1 0 4.001351 0.009195 0.031073	1475.0594*i* 11.0562 141.7098 221.3112 396.2477 407.1099 441.9579 579.6743 612.8714 624.4706 660.7408 695.5765 728.3560 841.8322 886.8618 945.4869 955.5820 1010.1689 1036.9696 1079.8284 1092.6894 1182.3454 1196.7554 1283.4329 1292.3063 1348.7928 1357.8446 1359.4246 1369.8862 1389.0109 1476.8577 1503.9766 1615.9626 1638.7173 3025.4594 3164.6641 3166.1855 3185.3734 3192.3185 3210.5100 3211.7971 3217.8827
C_6H_5-CH_4, TS2 (abst.)	6 0 0.031251 -1.214945 0.001094 6 0 1.430127 -1.210778 -0.000310 6 0 2.124973 -0.000497 -0.001016	1631.2038*i* 5.8999 77.5449 82.6487 365.0474 393.2251 396.5053 488.2791 527.2478

	6 0 1.431001 1.210301 -0.000308 6 0 0.032144 1.215481 0.001079 6 0 -0.633547 0.000502 0.001477 1 0 -0.515918 -2.151426 0.001770 1 0 1.973839 -2.149024 -0.000829 1 0 3.208574 -0.000891 -0.002156 1 0 1.975399 2.148150 -0.000816 1 0 -0.514383 2.152347 0.001728 6 0 -3.303563 0.000168 -0.000666 1 0 -3.593511 0.855991 -0.605498 1 0 -3.591797 -0.948674 -0.446817 1 0 -3.605794 0.090945 1.039643 1 0 -2.010726 0.001187 0.004870	618.4178 634.2324 673.6288 721.0411 840.3049 889.3387 948.2846 957.3946 1012.0094 1035.3507 1071.9120 1084.3134 1182.4712 1191.5091 1205.9087 1260.2175 1309.3524 1346.7893 1386.0855 1462.9699 1464.2549 1494.5596 1502.5772 1613.2616 1640.3232 3078.8693 3177.2574 3181.8477 3192.0885 3197.4966 3208.0325 3210.7238 3211.0268
$C_6H_5CH_3$	6 0 -0.195248 1.201640 0.009068 6 0 1.199061 1.204508 -0.002190 6 0 1.901952 0.000002 -0.008636 6 0 1.199065 -1.204506 -0.002190 6 0 -0.195245 -1.201642 0.009067 6 0 -0.912534 -0.000002 0.012617 6 0 -2.421052 -0.000001 -0.010180 1 0 -0.734616 2.143106 0.017771 1 0 1.735629 2.146310 -0.001902 1 0 2.985437 0.000004 -0.014406 1 0 1.735636 -2.146306 -0.001902 1 0 -0.734610 -2.143109 0.017771 1 0 -2.823715 -0.884212 0.487683 1 0 -2.796047 0.000086 -1.038180 1 0 -2.823715 0.884128 0.487830	37.8231 206.2712 342.3588 407.9360 465.7643 528.3220 635.8641 656.6401 731.3118 801.9039 848.8711 894.9721 952.2825 955.0482 1008.1685 1018.1595 1053.3691 1065.2558 1114.9837 1184.1882 1206.5717 1240.5602 1349.1282 1363.5999 1426.5846 1477.3594 1503.6366 1515.0100 1534.2986 1633.5091 1655.5264 3047.9870 3109.8765 3133.0242 3176.5428 3178.2715 3191.4570 3200.0783 3212.7948
CH_3	6 0 0.000000 0.000000 0.000000 1 0 0.000000 1.078881 0.000000 1 0 0.934338 -0.539441 0.000000 1 0 -0.934338 -0.539441 0.000000	481.6266 1426.5358 1426.5386 3136.5476 3320.3098 3320.3283

Table S2. Comparison of stationary point energies computed from high level explicitly correlated coupled cluster CCSD(T)-F12 wavefunction theory and the lower level density functional theory ωB97X-V/6-31+G* that is used for ab initio trajectory calculations. The reference energy is silane plus phenyl radical at infinite separation. The numbers are in agreement to 5 kJ mol^{-1}, which is close to the uncertainty of the wavefunction theory approach. (TS = transition state); energies are given in kJ mol^{-1}.

Method	Complex	Substitution TS	Abstraction TS	Substitution ΔE	Abstraction ΔE
Wavefunction Theory	-5	39	12	-30	-89
ωB97X-V/ 6-31+G*	-5	35	8	-26	-85

Table S3. Vibrational frequencies and geometrical parameters of the reactants, intermediates, products, and transition states involving Silane, at the ωB97X-V/6-31+G* level of theory.

Structure	Coordinates				Frequencies
C_6H_5	C	0.000000	0.000000	0.000000	403.50 427.28 599.20
	H	0.000000	0.000000	1.088629	617.54 675.70 731.17
	C	1.214435	0.000000	-0.692532	836.59 913.69 987.66
	H	2.156077	0.000000	-0.144532	992.55 1019.24 1038.36
	C	-1.214435	0.000000	-0.692532	1068.15 1092.40 1184.61
	H	-2.156077	0.000000	-0.144532	1191.30 1317.86 1331.31
	C	-1.228139	0.000000	-2.096050	1487.76 1501.78 1631.10
	H	-2.165026	0.000000	-2.650088	1682.63 3206.96 3214.12
	C	0.000000	0.000000	-2.722726	3227.89 3231.68 3238.05
	C	1.228139	0.000000	-2.096049	
	H	2.165026	0.000000	-2.650088	
SiH_4	Si	0.000000	0.000000	0.000000	930.78 931.27 933.78
	H	0.000000	0.000000	1.485457	987.95 989.75 2302.88
	H	1.400502	0.000000	-0.495152	2310.00 2310.35 2310.52
	H	-0.700251	1.212871	-0.495152	
	H	-0.700251	-1.212871	-0.495152	
	H	-2.156077	0.000000	-0.144532	
C_6H_5…SiH_4 complex	Si	0.003646	-0.001030	-0.000344	19.02 27.17 45.85
	H	0.015088	0.002516	1.484603	56.48 150.82 181.65
	H	1.395117	-0.008708	-0.521208	403.87 429.32 598.82
	H	-0.738360	-1.186481	-0.501830	619.17 677.70 732.46
	H	-0.680453	1.230454	-0.480813	836.41 914.08 917.61
	H	3.476919	-1.801166	0.858924	929.74 932.57 984.65
	C	2.901130	-2.683747	1.132447	987.81 989.87 992.99
	C	1.536677	-2.759180	0.951895	1020.31 1038.63 1068.24
	C	0.732969	-3.833997	1.266372	1092.32 1184.96 1190.94
	H	-0.342138	-3.827314	1.094783	1317.37 1331.50 1488.51
	C	1.375522	-4.950058	1.824486	1501.83 1630.57 1683.16
	H	0.791414	-5.829454	2.093752	2289.80 2298.81 2304.00
	C	2.757833	-4.935084	2.033923	2307.95 3206.79 3213.68
	H	3.246645	-5.806003	2.467226	3226.57 3229.94 3237.38
	C	3.518765	-3.813064	1.692089	
	H	4.595469	-3.811418	1.858750	
C_6H_5-SiH_4, TS1 (subst.)	Si	-0.000041	0.000128	-0.001719	571.87*i* 33.00 110.83
	H	0.006547	0.001590	1.496457	154.26 195.23 246.38
	H	1.301597	-0.000572	-0.745438	371.06 409.16 452.30
	H	-1.308088	-0.014268	-0.734065	621.39 676.31 699.44
	H	0.007894	-1.575511	-0.006158	747.74 815.53 833.97
	C	-0.011455	2.065532	-0.034386	865.15 937.24 972.96
	C	1.198611	2.757544	-0.027498	973.91 1002.27 1005.78
	H	2.147246	2.223749	-0.054749	1027.68 1048.79 1088.33
	C	-1.228950	2.744037	-0.010498	1111.92 1188.56 1217.22
	H	-2.171871	2.199700	-0.024490	1315.15 1353.87 1487.49

	C	-1.231228	4.142324	0.028221	1526.75 1655.76 1668.58
	H	-2.179520	4.678136	0.046053	1712.25 2169.93 2210.07
	C	-0.026433	4.847696	0.039524	2212.17 3206.33 3212.95
	H	-0.032314	5.936140	0.067040	3223.40 3228.36 3236.50
	C	1.185849	4.155805	0.011275	
	H	2.128273	4.702137	0.015819	
C_6H_5-SiH_4, TS2 (abst.)	Si	-0.004360	-0.001639	-0.002741	532.51*i* 34.98 47.98
	H	0.007513	0.002527	1.484320	56.01 262.16 296.83
	H	1.392821	-0.012109	-0.511881	402.78 433.78 446.22
	H	-0.718160	-1.212664	-0.489572	610.40 693.73 736.89
	H	-0.751934	1.285325	-0.531725	784.69 858.71 887.91
	C	-1.570203	2.607652	-1.112388	921.36 951.94 953.92
	C	-2.693896	2.377518	-1.886033	997.98 1000.26 1025.45
	H	-3.035273	1.366947	-2.109657	1025.64 1039.96 1055.88
	C	-1.090355	3.866229	-0.796089	1098.64 1104.33 1186.64
	H	-0.199731	4.000049	-0.182411	1197.47 1328.63 1336.72
	C	-1.791911	4.972504	-1.294169	1491.46 1517.14 1645.11
	H	-1.446636	5.980916	-1.067852	1682.00 2285.00 2297.57
	C	-2.932700	4.783602	-2.080119	2299.55 3201.23 3205.41
	H	-3.473391	5.647193	-2.464132	3215.39 3220.71 3233.69
	C	-3.384362	3.494146	-2.376584	
	H	-4.274367	3.355725	-2.989832	
$C_6H_5SiH_3$	Si	0.000112	-0.000051	0.000117	37.21 151.83 198.98
	H	0.015815	-0.007822	1.487754	391.43 405.62 434.20
	H	1.394802	0.007154	-0.517613	632.18 658.20 664.96
	H	-0.670176	1.250486	-0.450863	709.02 720.97 777.38
	C	-0.900581	-1.524222	-0.633078	887.42 945.14 955.91
	C	-1.948506	-2.103227	0.102296	959.76 976.87 1014.75
	H	-2.232796	-1.682507	1.067709	1022.27 1034.36 1066.96
	C	-2.636374	-3.219311	-0.377936	1117.80 1154.94 1191.48
	H	-3.444921	-3.653300	0.208711	1229.56 1311.19 1371.35
	C	-2.284290	-3.779687	-1.607349	1488.11 1549.13 1665.45
	H	-2.817932	-4.651633	-1.983003	1689.66 2281.36 2286.49
	C	-1.242761	-3.221949	-2.351209	2291.78 3195.28 3196.20
	H	-0.960604	-3.658201	-3.308458	3212.05 3222.97 3234.46
	C	-0.558667	-2.105809	-1.865451	
	H	0.256908	-1.687327	-2.456613	
C_6H_6	C	0.000000	0.000000	0.000000	414.28 414.41 619.98
	H	0.000000	0.000000	1.089101	620.07 696.81 722.51
	C	1.209785	0.000000	-0.698461	882.08 882.16 1009.98
	H	2.152970	0.000000	-0.153908	1010.10 1021.53 1034.80
	C	1.209785	0.000000	-2.095394	1039.30 1078.95 1079.02
	H	2.152970	0.000000	-2.639946	1178.75 1211.19 1211.37
	C	0.000000	0.000000	-2.793854	1339.57 1391.84 1539.18
	H	0.000000	0.000000	-3.882955	1539.35 1690.65 1690.73
	C	-1.209785	0.000000	-0.698461	3202.89 3212.47 3212.54

	H	-2.152970	0.000000	-0.153908	3228.44 3228.52 3238.70
	C	-1.209785	0.000000	-2.095394	
	H	-2.152970	0.000000	-2.639946	
SiH_3	Si	0.000000	0.000000	0.000000	785.66 946.08 949.89
	H	0.000000	0.000000	1.487703	2266.95 2300.49 2300.85
	H	1.389887	0.000000	-0.530580	
	H	-0.770366	-1.156859	-0.530580	

Table S3. Anharmonic correction to the barrier for the silane substitution pathway. All energies are in kJ mol^{-1} and all zero point energies (ZPEs) were calculated at geometries that correspond to local extrema for the method employed. B2PLYP-D3 ZPEs are also provied for comparison to the more approximate B3LYP results.

Species	Harmonic ZPE (B3LYP/6-311G**)	TOSH ZPE (B3LYP/6-311G**)	Anharmonic contribution	Harmonic ZPE (B2PLYP/6-311G**)
Silane	81.92	79.61	-2.31	83.55
Phenyl radical	228.36	224.08	-4.28	229.36
Transition state	306.90	299.02	-7.82	308.29

Movie M1. Visualization of a 0.4 ps segment of a QCT trajectory showing the substitution of atomic hydrogen by a phenyl radical in silane.

Movie M2. Visualization of a 0.3 ps segment of a QCT trajectory showing the abstraction of atomic hydrogen from silane by a phenyl radical.